HORIZON 2020

HORIZON 2020 RESEARCH AND INNOVATION FRAMEWORK PROGRAMME OF THE EUROPEAN ATOMIC ENERGY COMMUNITY

Nuclear Fission and Radiation Protection 2018 (NFRP-2018-4)

Project acronym:	**SANDA**
Project full title:	**Solving Challenges in Nuclear Data for the Safety of European Nuclear facilities**
Grant Agreement no.:	**H2020 Grant Agreement number: 847552**

Workpackage N°:	***WP5***
Identification N°:	
Type of document:	***Non-contractual report***
Title:	***Homogenized neutronics model of MYRRHA design revision 1.8***
Dissemination Level:	***PP***
Reference:	***SCK CEN/44767116***
Status:	***VERSION 1.2***
Comments:	

	Name	Partner	Date	Signature
Prepared by:	L. Fiorito A. Hernandez-Solis P. Romojaro	SCK CEN	19-11-2021	
WP leader:	R. Jacqmin	CEA		
IP Co-ordinator:	E. González	CIEMAT		

Table of content

Glossary of abbreviations

ACE	A Compact Endf
ACS	Above-Core Structure
ADS	Accelerator-Driven System
BoC	Beginning-of-Cycle
BoL	Beginning-of-Life
CDT	Central Design Team for a Fast-spectrum Transmutation Experimental Facility
CHANDA	solving CHAllenges in Nuclear DAta
CR	Control Rod
EoC	End-of-Cycle
EUROTRANS	EUROpean Research Programme for the TRANSmutation of High Level Nuclear Waste in an Accelerator Driven System
FA	Fuel Assembly
IPS	In-Pile Section
JEFF	Joint Evaluation Fission and Fusion
LBE	Lead-Bismuth Eutectic
MOX	Mixed Oxide
MYRRHA	Multi-purpose Hybrid Research Reactor for High-tech Applications
SANDA	Supplying Accurate Nuclear Data for energy and non-energy Applications
SR	Safety Rod
STA	Spallation Target Assembly
S/U	Sensitivity and Uncertainty
WP	Work Package

Version control

- 16/11/2021: A mistake was found in the homogenization process: Fe added was missing in material 15-15Ti. Moreover, 15-15Ti was used as wrapper material instead of T91. Homogenization has been re-calculated and MCNP input and Section 5 of this report have been updated accordingly.

Abstract

The MCNP neutronics model referring to the MYRRHA reactor design version 1.8 was homogenized at the assembly level as a part of the SANDA WP5. The model description, homogenization assumptions and methodology are reported, as well as a comparison of the model performances with respect to the heterogeneous model.

Keywords

MYRRHA; neutronics model; homogenization; SANDA; MCNP; OpenMC

1. Introduction

In 1997 SCK CEN launched the MYRRHA (*Multi-purpose hYbrid Research Reactor for High-tech Applications*) project [1], with the goal of designing a multi-purpose flexible irradiation facility that could replace the BR2 reactor and provide a research ground for Accelerator Driven System (ADS) applications. MYRRHA was conceived as a pool-type ADS reactor with a proton accelerator linked to a subcritical core fueled with MOX and cooled by lead-bismuth eutectic (LBE), with the chain reaction guaranteed by the proton beam interaction with the LBE spallation target.

The MYRRHA concept, in its 2005 version, was offered as a design basis for the XT-ADS system within the EU-FP6 EUROTRANS (EUROpean Research Programme for the TRANSmutation of High Level Nuclear Waste in an Accelerator Driven System) project [2] in the context of partitioning and transmutation. In a later stage, a small-scale reactor called MYRRHA/XT-ADS was developed, with an optimization of the design choices based on the XT-ADS needs.

As an upgrade of MYRRHA/XT-ADS, MYRRHA/FASTEF was developed within the EU-FP7 CDT (Central Design Team for a Fast-spectrum Transmutation Experimental Facility) project [3]. Compared to its predecessor, both sub-critical and critical operation modes were requested. Within the CDT project the reactor was designed to an advanced engineering level with the following objectives in mind: being a high-flux and flexible fast spectrum irradiation facility, being an effective demonstrator of the ADS technology for high level waste transmutation, and being a demonstrator of the lead fast reactor technology [4][5].

A further core revision was delivered in 2014 with the name "MYRRHA Revision 1.6"[6]. This version addressed the shortcomings of the CDT work, including the rather low expected fuel discharge burnup and the concerns regarding the use of 34.5 wt.%-enriched MOX. The outcome was a larger core that could operate both in critical and subcritical modes at 100 and 70 MWth, respectively. The fuel enrichment was also changed to 30 wt.% plutonium.

New design constraints identified after the version 1.6 finalization, together with the need for a core size reduction, led to a further upgrade of the core design called "version 1.8".

Simplified, homogenized on fuel assembly level, models for version 1.6 [7] were developed and used as a basis for the Sensitivity and Uncertainty (S/U) analyses performed within the work package (WP) 10 of the EU-FP7 CHANDA (solving CHAllenges in Nuclear DAta) project [8,9]. The objective of these studies was to identify and improve the most important nuclear data for neutron induced reactions for the effective neutron multiplication factor, k_{eff}, and effective delayed neutron fraction, β_{eff}, of MYRRHA. As a result, recommendations to the JEFF project were given [10], which were included in the latest version of the JEFF nuclear data library, JEFF-3.3 [11].

Within the context of the SANDA (Supplying Accurate Nuclear Data for energy and non-energy Applications) H2020 project WP5, SCK CEN has produced simplified versions of the MYRRHA reactor reference neutronics models for the latest neutronics design version 1.8 [12]. The core and reactor components were homogenized radially at the assembly level and vertically on a number of discrete regions. In-vessel reactor components located outside the core barrel, such as primary pumps, primary heat exchangers, fuel handling machines and fuel storages, were neglected and not modelled. Nuclide composition, densities and temperatures of the several materials were homogenized for each region using the corresponding volumes as a weighting function. The models will be used in task 5.1 to perform S/U analyses of the latest MYRRHA design, focusing on the reactivity coefficients (i.e., Doppler and coolant density coefficients). This will allow further identifying MYRRHA-related nuclear data in need for improvement, which will be communicated to the JEFF community for consideration in the next release of the JEFF nuclear data library, JEFF-4, planned for 2024 [13].

An input deck containing the details of both the critical and subcritical reactor model was created and is distributed along with the present report:

- **myr18_bol.i**: the MYRRHA reactor at beginning-of-life modelled with MCNP.

2. Neutronics models

Detailed heterogeneous 3D geometrical models of the MYRRHA reactor both for the critical and subcritical layouts are developed at SCK CEN to reproduce a realistic design of the facility. The Monte Carlo N-particle transport code MCNP version 6.2 [14] is customarily adopted at SCK CEN as a reference for the MYRRHA neutronics calculations. The neutronics models are representative of:

- the reactor start-up conditions at beginning-of-life (BoL) where only fresh fuel is loaded in the core;
- a hypothetical irradiation cycle in a dynamic equilibrium state that is reached after the reactor operation at constant nominal power.

Computer calculations using high-quality codes such as ALEPH-2 [15] and MCNP-6.2 were used to produce a neutronics model of the reactor for its long-term operation at nominal power (beginning-of-cycle BoC and end-of-cycle EoC). A cycle-by-cycle loading/unloading and in-core (re)shuffling of the fuel assemblies (FAs) was incorporated in the model. Fuel reloading involves removing (partially) depleted or used FAs from the shutdown core and replacing them with fresh fuel. Then the fuel still in the core is reshuffled. The reloading of FAs in the MYRRHA core requires recalculating the core reactivity, the power distribution, and the nuclide inventory of the fuel at every irradiation cycle to guarantee constant irradiation performances over the reactor lifetime within the safety requirements and design constraints. Together with this report only the BoL models are distributed, not the BoC and EoC models.

JEFF-3.1.2 [16] was selected as a reference nuclear data library for the MYRRHA calculations [17]. Neutron-induced nuclear data evaluated files were processed at SCK CEN into the MCNP-compatible format ACE over the whole range of temperatures reported in the MYRRHA model [18]. The library is not distributed.

To perform proton source-driven calculations for the subcritical core the CEM03.03 event generator [19] incorporated in MCNP-6.2 was used to transport high-energy particles for energy ranges above 200 MeV and for nuclides not covered by tabulated nuclear data libraries [20]. The 600 MeV proton beam originates 115 cm above the fuel column mid-plane and descends vertically in the core central assembly with a Gaussian shape swept around the beam axis [21]. The proton beam radial profile is shown in Figure 1.

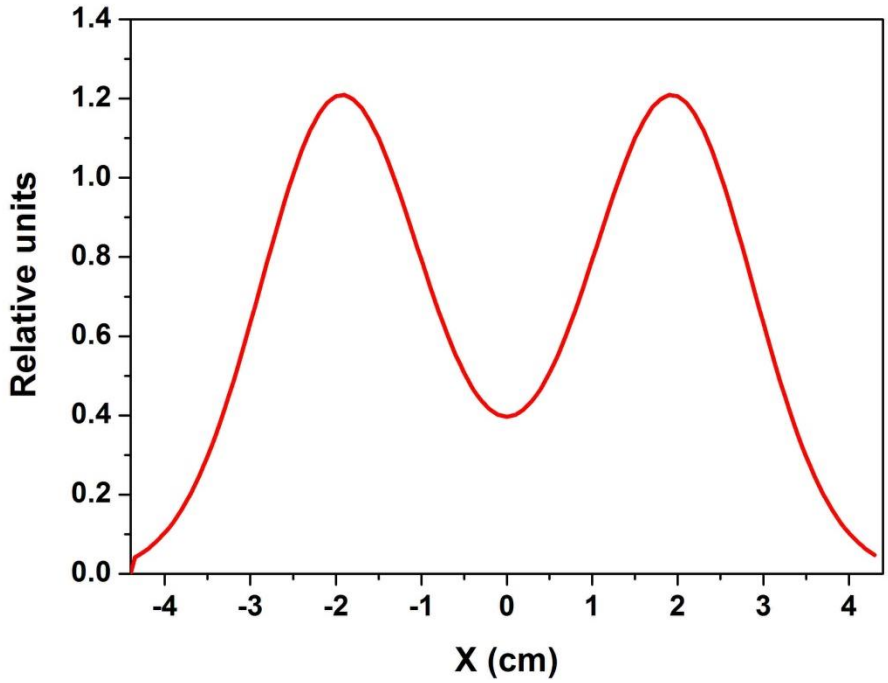

Figure 1: Proton beam radial profile [21].

3. Critical and subcritical core layout

The simulated MYRRHA core configurations include 163 assemblies/channels arranged in a hexagonal lattice with a central position and seven radial crowns. The assembly lattice is shrouded by a stainless steel jacket and wrapped by a cylindrical core barrel with an inner diameter of 157.0 cm and a wall thickness of 3.0 cm. The seventh crown does not contain corner assemblies to comply with the geometrical constraint imposed by the core barrel dimensions.

Both the critical and subcritical layout include:

- hexagonal fuel assemblies (FAs) consisting of 127 fuel elements with highly enriched MOX fuel. Each fuel element contains a fuel vertical column 65.0 cm long that defines the axial center of the model;
- boron carbide B_4C control rod (CR) bundles;
- in-pile sections (IPSs) for material testing and experiments with fast neutron fluxes;
- in-pile sections for the production of molybdenum-99, also called thermal islands;
- dummy assemblies filled with LBE;
- reflector assemblies with bundles of magnesium oxide rods.

A spallation target assembly (STA) is located in the central channel of the subcritical core layouts and hosts the accelerator proton beam tube and window. Safety rods (SRs) are included in the critical layout as a redundant and diversified emergency shutdown system that is complementary to the CRs.

Table 1: Assembly types modelled in the hexagonal lattice of the MYRRHA core.

Assembly	Subcritical BoL	Subcritical BoC	Critical BoL	Critical BoC
STA	1	1	-	-
FA	54	78	69	105
Fast IPS	6	6	1	1
Thermal islands	3	3	6	6
CR	3	3	6	6
SR	-	-	3	3
Dummy	54	30	36	-
Reflector	42	42	42	42

Each core assembly/channel in the neutronics model extends vertically from the horizontal plane defining the bottom of the core barrel – i.e. 147.5 cm below the fuel column mid-plane – and up to the reactor cover. The reactor core is vertically connected to the reactor cover by an above core structure (ACS). The model is vertically truncated at its top-end in correspondence of the hot LBE free surface level, i.e. 290.0 cm above the fuel column mid-plane. Below the core the model is simplified by only accounting for the presence of LBE. The model is vertically truncated at its bottom-end 554.6 cm below the fuel column mid-plane. The reactor pool model outside the core barrel is largely simplified. No component of the primary system such as the pumps and the heat exchangers, as well as the structural components such as the reactor vessel and cover, and the fuel handling machines and fuel storages are modelled. The model is radially truncated 760.0 cm equidistantly from the radial center.

The radial layouts of the homogenized critical and subcritical MYRRHA core models at BoL are reported in Figure 2.

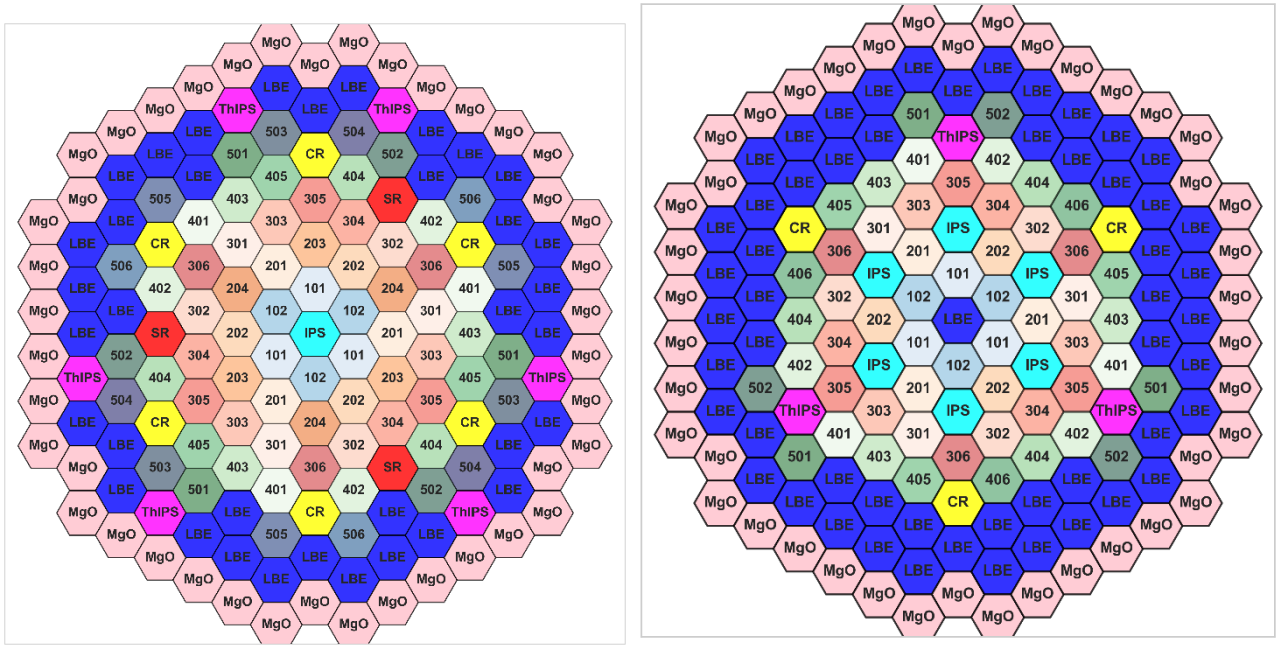

Figure 2: Radial view of the MYRRHA homogenized critical (left) and subcritical (right) core at BoL.

In Figure 2 the following nomenclature was adopted:

- **LBE**: hexagonal dummy-channel filled by lead bismuth eutectic (in the subcritical layout the central channel is also named **LBE** despite the presence of the beam tube and window);
- **CR**: channel containing the control rod bundle;
- **SR**: channel containing the safety rod bundle;
- **IPS**: in-pile section for irradiation experiments;
- **ThIPS**: in-pile section for radioisotope production (thermal islands);
- **MgO**: reflector channel composed of reflector pins in magnesium oxide (MgO);
- **101-608**: fuel assemblies (FAs) grouped in batches.

The FA subdivision into batches follows the core 1/3rd azimuthal symmetry around the central assembly, making each batch be composed of three FAs. Each batch is identified by a three digit number, i.e. XYY, where the first digit – i.e. X – indicates the core radial crown (or ring) where the FA is located, and the second and third digits – i.e. YY – represent a counter with an increasing order to distinguish batches with different burnup levels (the counter increases with burnup).

The axial layout of the homogenized critical MYRRHA core model at BoL is reported in Figure 3.

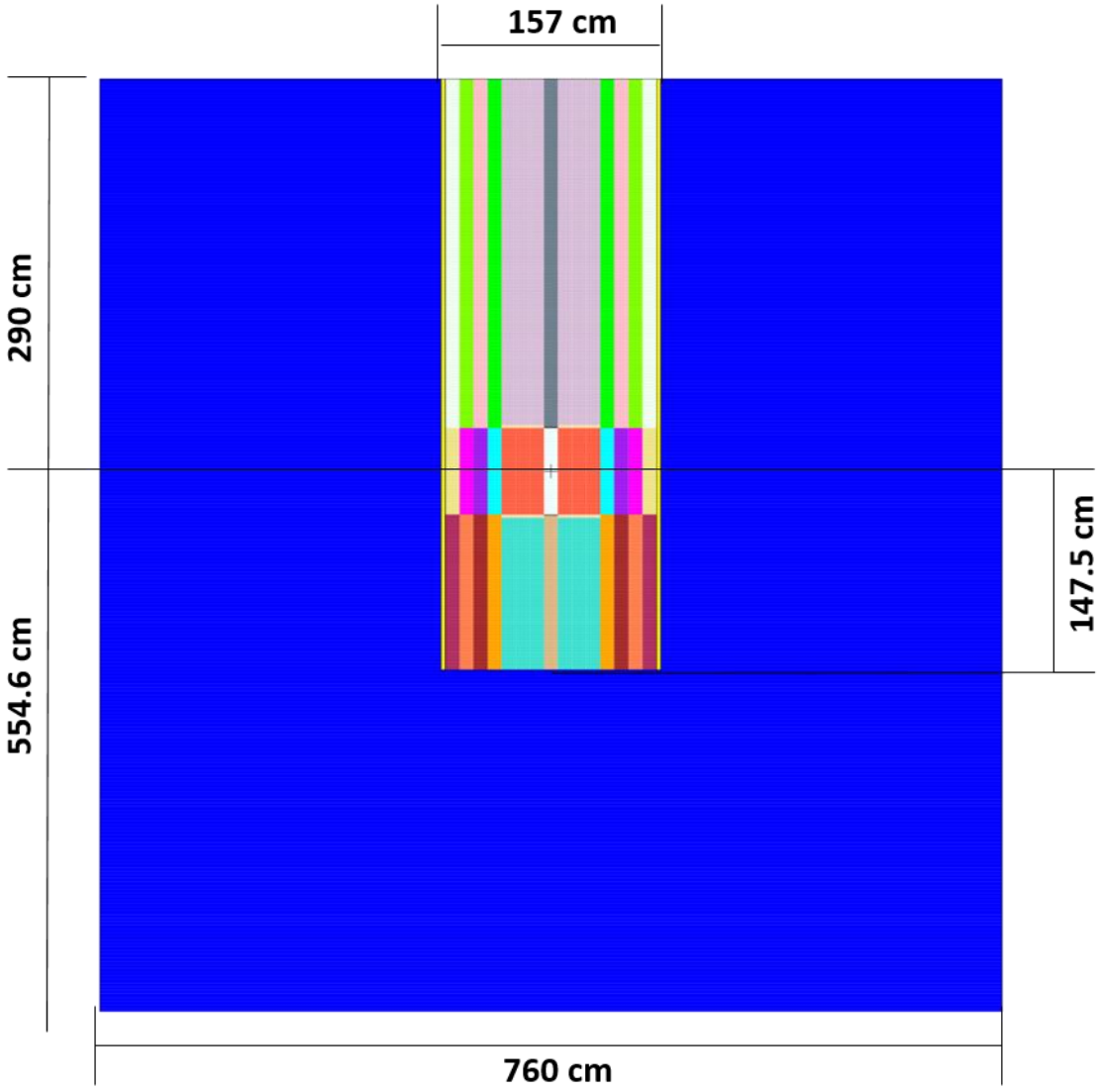

Figure 3: Axial view of the MYRRHA homogenized critical core at BoL.

4. Model homogenization

The core model was radially homogenized at the assembly level and axially in either two, three or five zones. Nuclide atomic compositions were homogenized using the corresponding material volumes as weighting functions, as

$$\langle N_j \rangle = \frac{\sum_i V_i N_{i,j}}{\sum_i V_i} \quad (1)$$

where:

- $N_{i,j}$ is the atomic composition in atoms/cm/b of nuclide j in material i;
- V_i is the volume of material i in cm^3 in the selected homogenization region;
- $\langle N_j \rangle$ is the atomic composition in atoms/cm/b of nuclide j averaged over the volume of all materials in the selected homogenization region;

Then, the volume-averaged material atomic density $\langle \rho \rangle$ is the sum of all nuclide compositions $\langle N_j \rangle$ included in the homogenization region,

$$\langle \rho \rangle = \sum_j \langle N_j \rangle \quad (2)$$

Analogously, the volume-averaged material temperature $\langle T \rangle$ is

$$\langle T \rangle = \frac{\sum_i V_i T_i}{\sum_i V_i} \quad (3)$$

and it was rounded off to a set of pre-defined temperature values in a range with uniform intervals of 50 degrees [22].

Volumes and homogenized atomic compositions were calculated using the OpenMC code [23,24]. OpenMC is an open source Monte Carlo neutron and photon transport simulation code, developed with a focus on high-performance algorithms and modern software development practices. It is capable of performing fixed source, k-eigenvalue, and subcritical multiplication calculations, as well as depletion calculations, on models built using either a constructive solid geometry or CAD representation. OpenMC also has the capability to stochastically determine volumes of cells, materials and universes. First, core models for both configurations were developed based on the MCNP heterogeneous models [25]. Then, stochastic volume calculations were carried out with OpenMC to determine the volume with a statistical uncertainty lower than 0.05% for each cell of the models. The calculated volumes where integrated in the above equations to calculate the averaged quantities.

The hexagonal fuel assembly (FA) consisting of 127 fuel pins containing highly enriched MOX fuel was split into five axial parts:

- a central part covering the whole 65 cm of the fuel column (active part);
- a 3.5 cm-long cylindrical lower insulation/reflector segment in yttria stabilized zirconia placed above the active zone;
- a 3.5 cm-long cylindrical upper insulation/reflector segment in yttria stabilized zirconia placed below the active zone;
- everything above the upper insulator/reflector segment;
- everything below the lower insulator/reflector segment.

In the neutronics models the active part is vertically symmetric with respect to the system origin. Then, the fuel column extends from -32.5 cm below the origin to 32.5 cm above the origin. The homogenized fuel assembly is displayed in Figure 4.

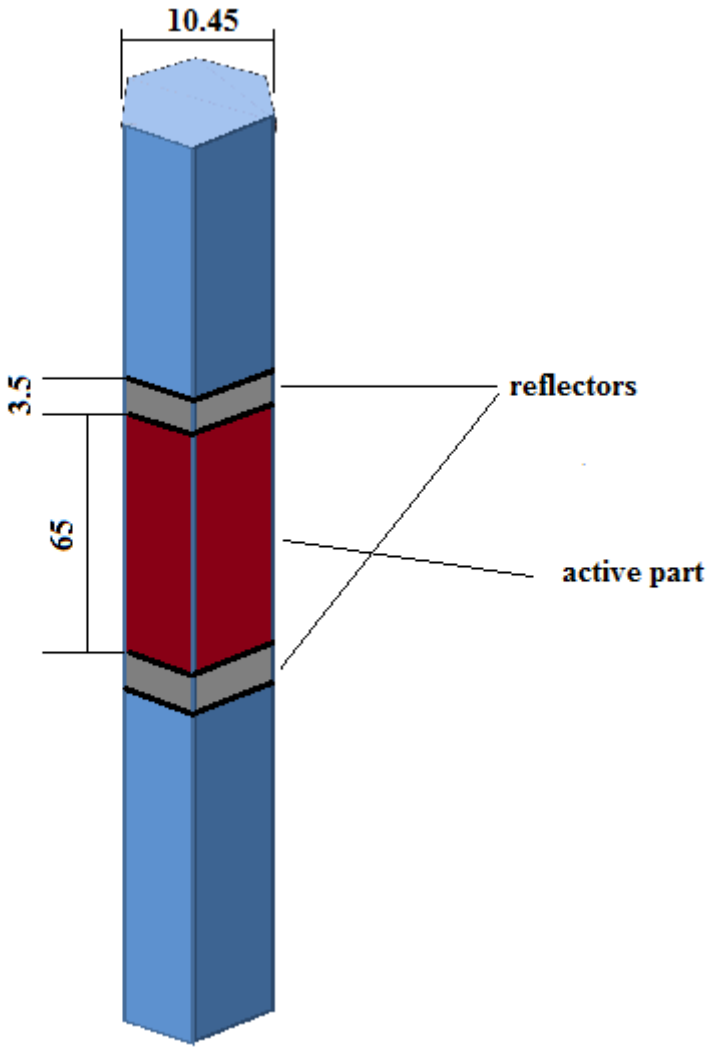

Figure 4: Homogenized fuel assembly vertical layout. Dimensions are given in cm.

Given that each hexagonal assembly has a pitch of 10.45 cm, corresponding to an area of $A = 94.57$ cm^2, then the volume of each axial segment can be calculated multiplying the area by the segment height h,

$$V = A \times h \qquad 4$$

The volume fractions for the different materials present in the active zone of a fuel assembly are reported in Table 2.

Table 2: Volume fractions used for the homogenization of the active part of a fuel assembly.

Material	Volume fraction (%)
MOX	30.98
Cladding	14.81
Wrapper	7.29
Helium gap	2.69
LBE	44.23

The in-pile sections for material testing, the thermal islands, the reflector assemblies, the control rods and the safety rods were axially split into three parts:

- a central part covering the whole 65 cm of the fuel column (active part);
- everything above the active zone;
- everything below the active zone.

The spallation target assembly was split into two axial parts:

- above the lowest point of the beam window external wall, with a partial homogenization of the LBE and wrapper;
- below the lowest point of the beam window external wall.

The lowest point of the beam window was determined to be located 7.585 cm above the fuel column mid-plane. The beam window's position was optimized to improve the neutronics performances of the subcritical core driven by the 600-MeV proton beam [21].

The stainless steel jacket is modelled as subdivided into hexagonal lattice as for all other core components. The axial discretization is in three zone equivalent to those of the other assemblies without fuel.

Table 3 reports the homogenized regions and their main characteristics used to create the homogenized core layouts.

Table 3: Volume, density and temperatures of the homogenized regions.

		Area (cm^2)	Height (cm)	Volume (cm^3)	Density (at/b/cm)	Temperature (K)
FA	Top	94.57	254	24020.78	3.743639E-02	600
	Upper reflector	94.57	3.5	331.00	3.685324E-02	700
	Middle	94.57	65	6147.05	5.403043E-02	800
	Lower reflector	94.57	3.5	331.00	3.685324E-02	700
	Bottom	94.57	111.5	10544.56	4.603599E-02	600
IPS	Top	94.57	257.5	24351.78	4.711608E-02	600
	Middle	94.57	65	6147.05	4.403813E-02	650
	Bottom	94.57	115	10875.55	3.089478E-02	600
Thermal island	Top	94.57	257.5	24351.78	7.753268E-02	300
	Middle	94.57	65	6147.05	7.823904E-02	300
	Bottom	94.57	115	10875.55	4.257130E-02	300
CR	Top	94.57	257.5	24351.78	3.633771E-02	600
	Middle	94.57	65	6147.05	2.915689E-02	650
	Bottom	94.57	115	10875.55	4.007714E-02	600
SR	Top	94.57	257.5	24351.78	5.197334E-02	600
	Middle	94.57	65	6147.05	4.322105E-02	650
	Bottom	94.57	115	10875.55	4.201838E-02	600
Dummy	Top	94.57	257.5	24351.78	3.719197E-02	600
	Middle	94.57	65	6147.05	3.403032E-02	650
	Bottom	94.57	115	10875.55	4.301951E-02	600
Reflector	Top	94.57	257.5	24351.78	3.776276E-02	600
	Middle	94.57	65	6147.05	7.781197E-02	650
	Bottom	94.57	115	10875.55	6.715429E-02	600
STA	LBE + wrapper	-	282.415	9990.69	4.787238E-02	600
	Bottom	94.57	155.085	14666.39	3.403028E-02	600
SS jacket	Top	94.57	257.5	24351.78	6.353354E-02	600
	Middle	94.57	65	6147.05	8.491454E-02	600
	Bottom	94.57	115	10875.55	8.491454E-02	600

The spallation target beam tube and window are made of Ferritic Martensitic Steel FMS T91 with a density of 7.760 g/cm^3 and a temperature of 600 K. Outside the core barrel (and below the core) LBE with 55.5 wt.% Bi and 45.5 wt.% Pb is modelled as the reactor coolant. Volume-averaged temperature and density of, respectively, 550 K and 10.44 g/cm^3 are provided.

5. Comparison of heterogeneous and homogenized models

A comparative analysis of the reference heterogeneous model and the homogenized model was performed with MCNP. The following neutronics parameters are reported:

- the effective neutron multiplication factor k_{eff};
- the ratio of normalized neutron flux per fuel assembly batch;
- the normalized neutron spectra in several reactor assemblies and in the core.

Table 4: Comparison of the neutron multiplication factor k_{eff} (with statistical error σ) calculated for the homogeneous and heterogeneous MYRRHA models. Results refer to a configuration with CR fully extracted.

	Subcritical heterogeneous	homogeneous	Critical heterogeneous	homogeneous
$k_{eff} \pm \sigma$	0.93247± 0.00029	0.93634 ± 0.00027	1.01458 ± 0.00027	1.01512 ± 0.00029

The normalized neutron flux are given as a ratio with respect to the reference values calculated for the heterogeneous core. Results are provided in Table 5.

Table 5: Ratio of the normalized integral neutron flux calculated in the homogeneous and heterogeneous core per FA batch and over the active length. The FA batch nomenclature refers to Figure 2.

FA batch	subcritical	critical
101	1.00	1.00
102	1.00	1.00
201	1.00	1.00
202	1.00	1.00
203	-	1.00
204	-	1.00
301	1.00	1.00
302	1.00	1.00
303	1.00	1.00
304	1.00	1.00
305	1.00	0.98
306	0.98	0.99
401	1.00	0.99
402	1.00	1.00
403	1.00	1.00
404	1.00	0.99
405	0.99	0.98
406	0.99	-
501	1.01	1.00
502	1.00	1.01
503	-	1.02
504	-	1.02
505	-	1.02
506	-	1.03

Calculations for the subcritical model were run using the reference configuration with an external source, except for the subcritical k_{eff} calculation which was performed using the criticality source (KCODE card in MCNP).

5.1. Critical core

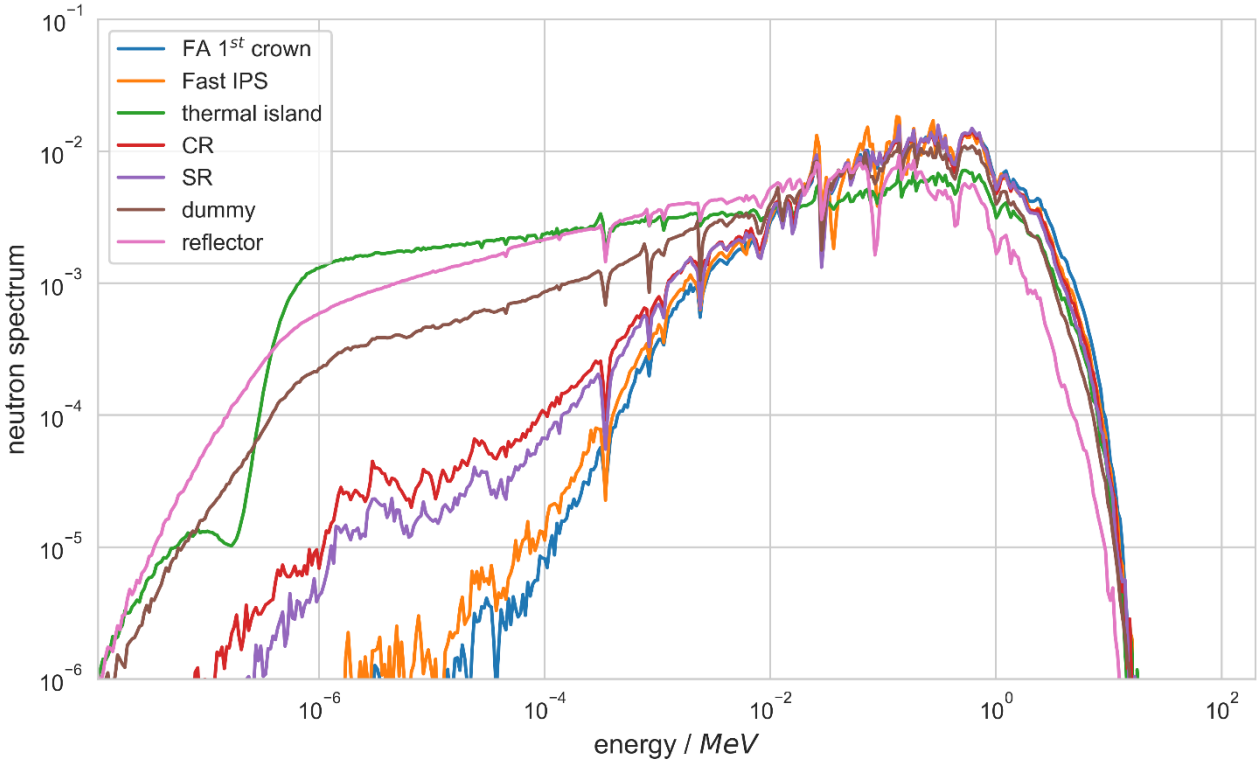

Figure 5: Normalized neutron spectra calculated for the MYRRHA critical BoL homogeneous model in several reactor components averaged over the active zone.

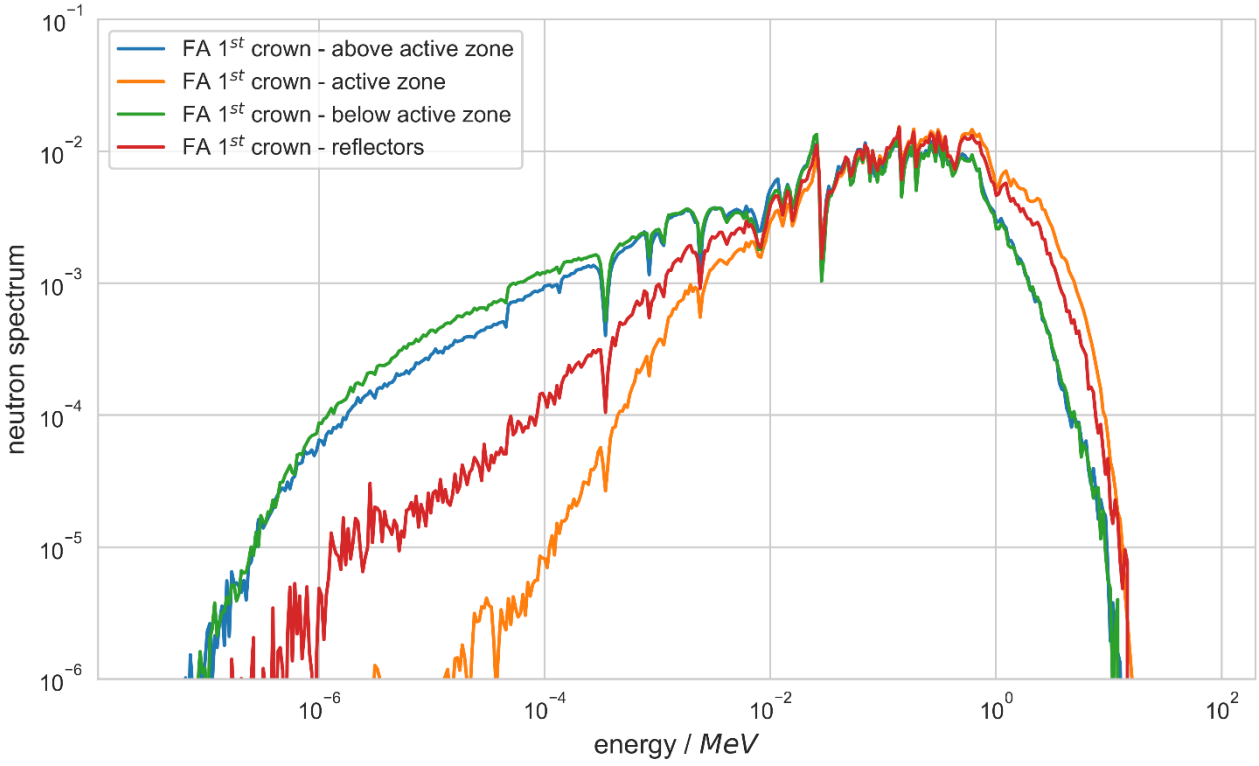

Figure 6: Normalized neutron spectra calculated for the MYRRHA critical BoL homogeneous model in a FA in the first crown (batch 101) and averaged over different axial zones.

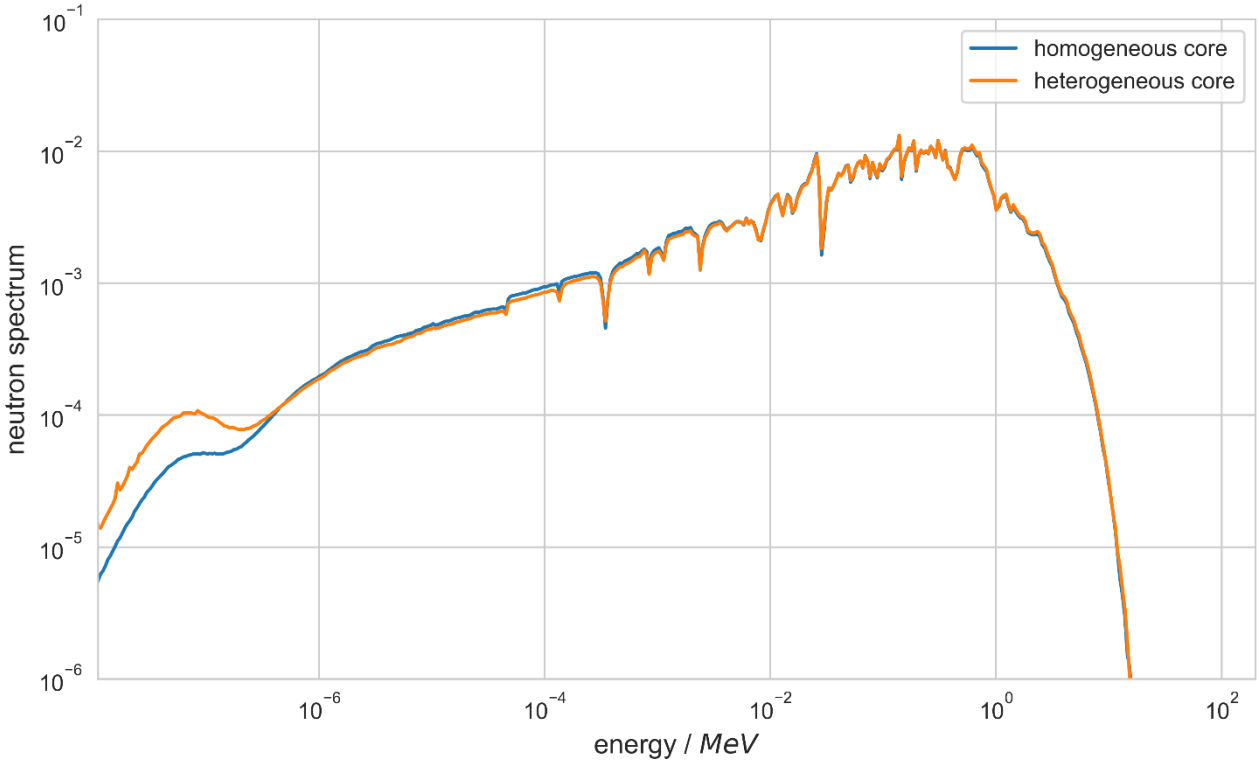

Figure 7: Normalized neutron spectra calculated for the MYRRHA critical BoL homogeneous model over the whole core.

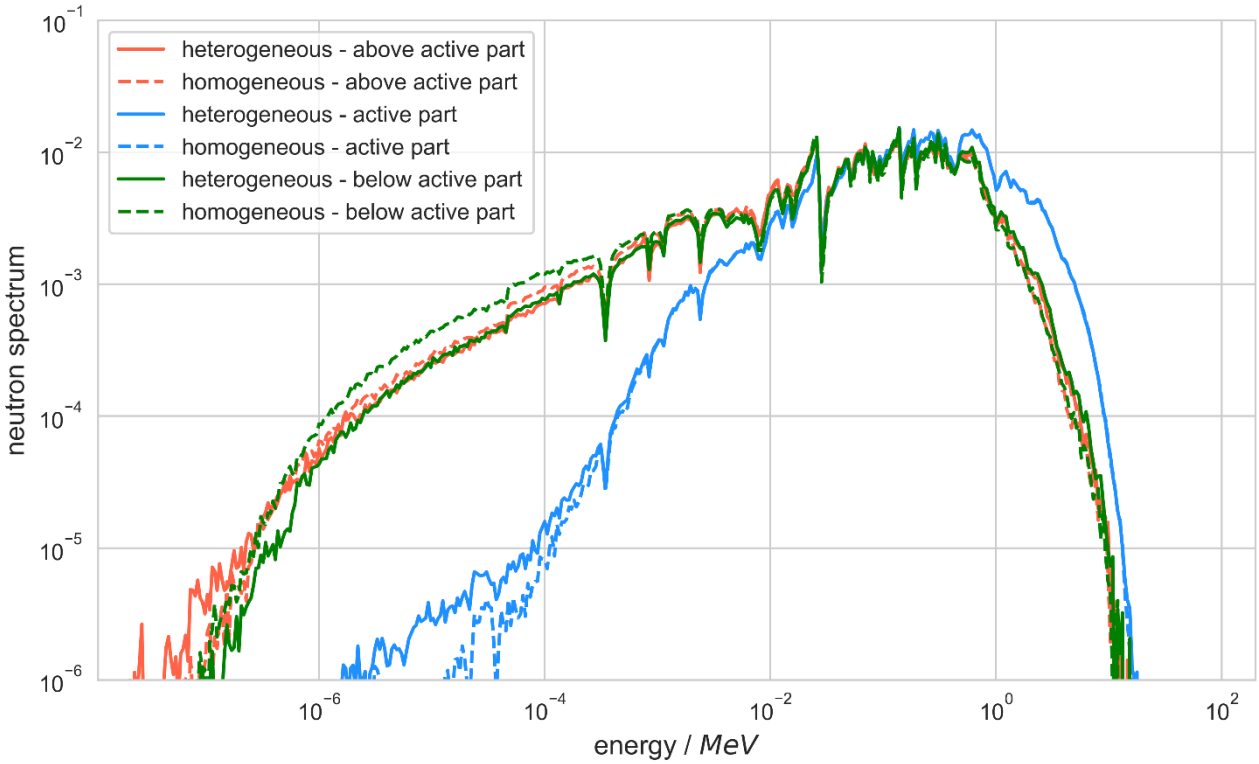

Figure 8: Comparison of the normalized neutron spectra calculated for the MYRRHA critical BoL homogenous and heterogeneous models in a FA in the first crown (batch 101) and averaged over different axial zones.

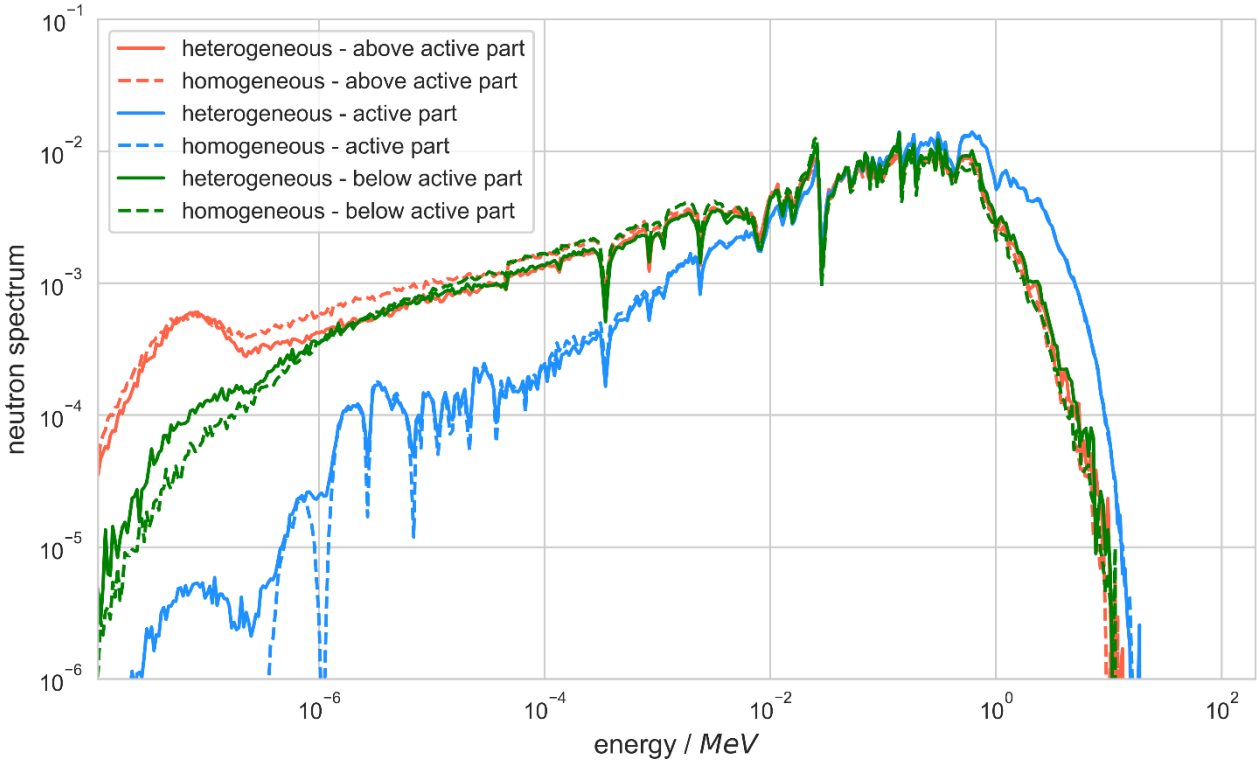

Figure 9: Comparison of the normalized neutron spectra calculated for the MYRRHA critical BoL homogenous and heterogeneous models in a FA in the fifth crown (batch 501) and averaged over different axial zones.

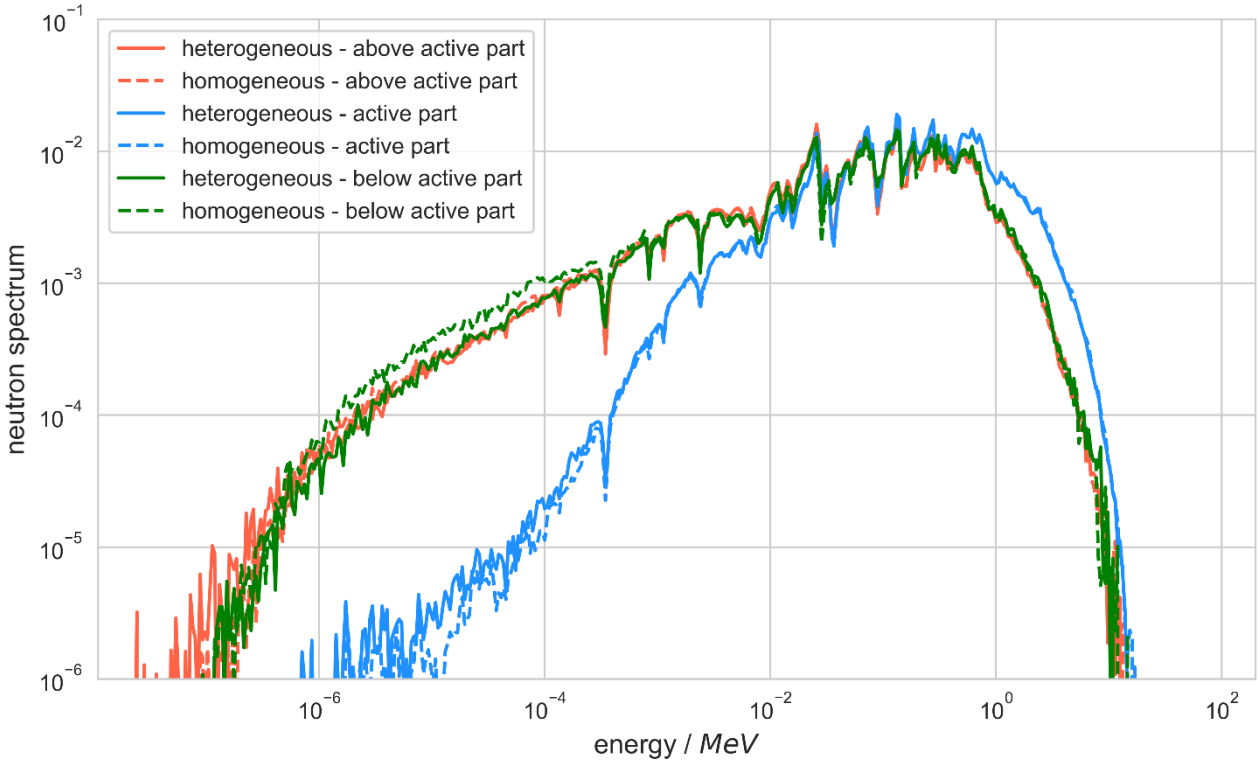

Figure 10: Comparison of the normalized neutron spectra calculated for the MYRRHA critical BoL homogenous and heterogeneous models in a fast IPS and averaged over different axial zones.

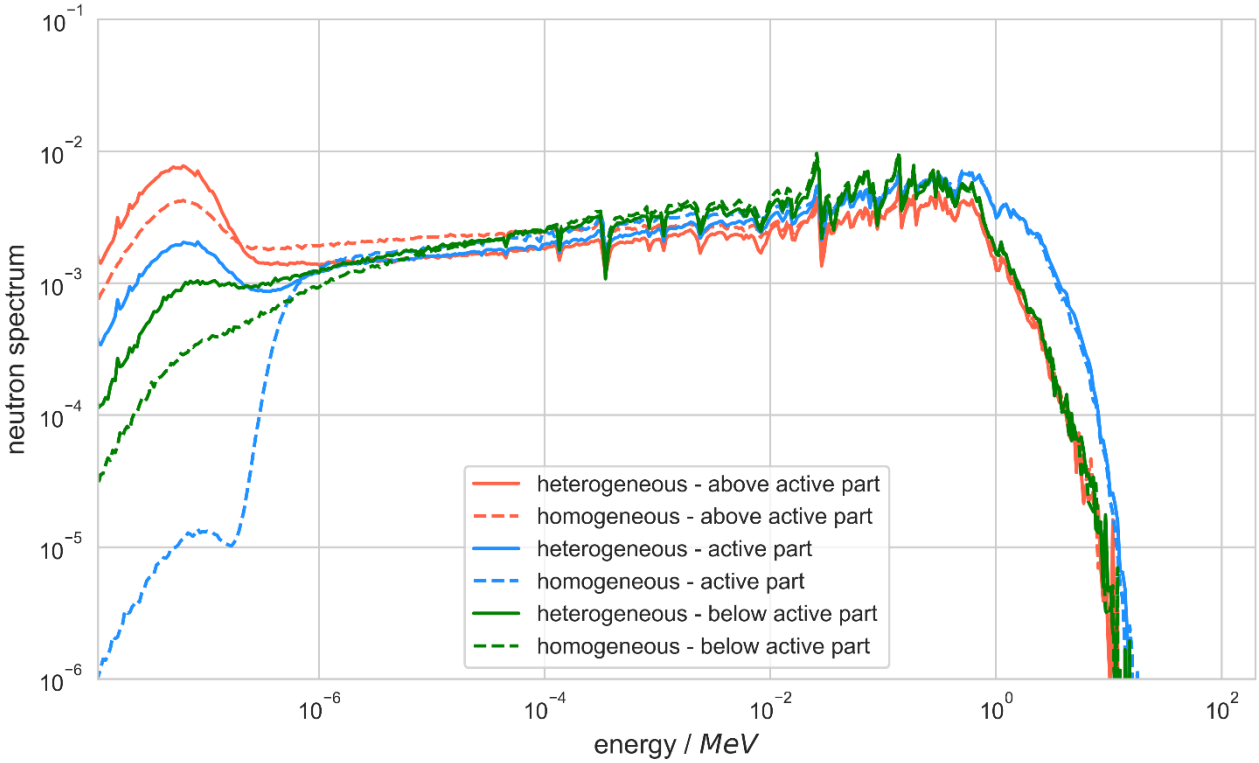

Figure 11: Comparison of the normalized neutron spectra calculated for the MYRRHA critical BoL homogenous and heterogeneous models in a thermal island and averaged over different axial zones.

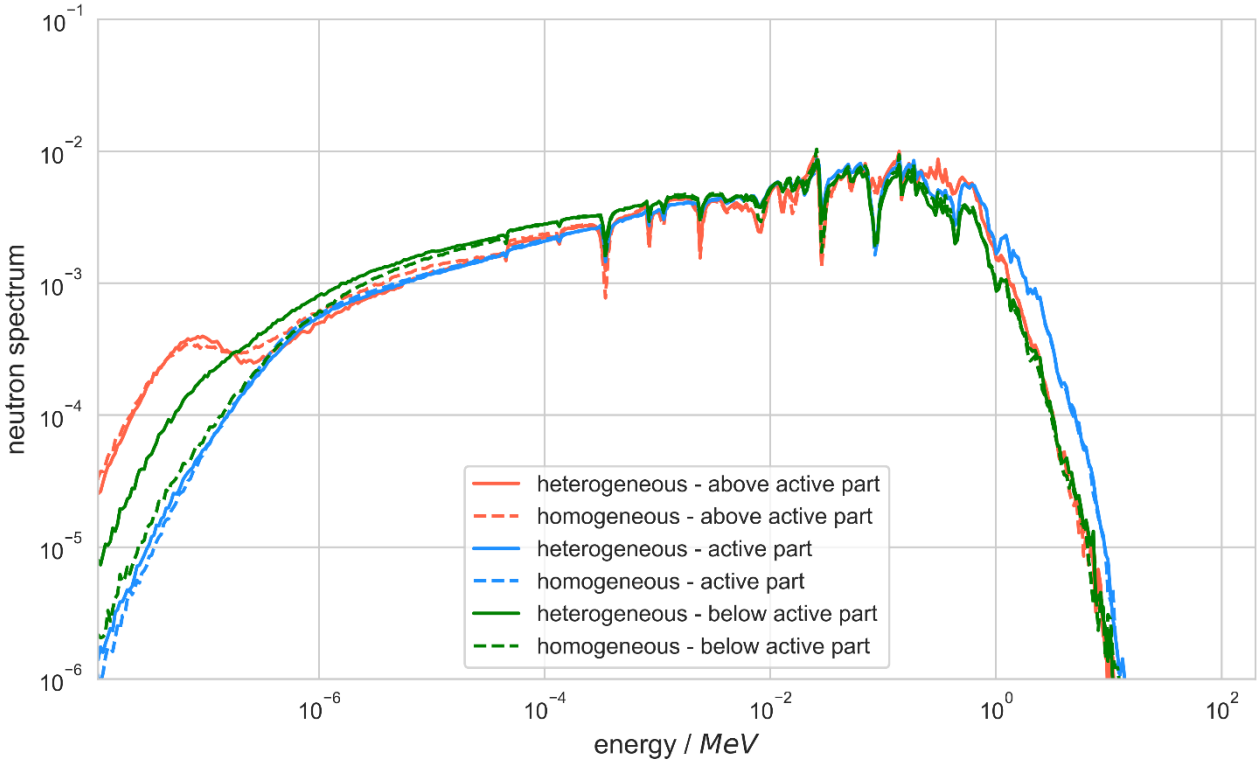

Figure 12: Comparison of the normalized neutron spectra calculated for the MYRRHA critical BoL homogenous and heterogeneous models in a reflector assembly and averaged over different axial zones.

5.2. Subcritical core

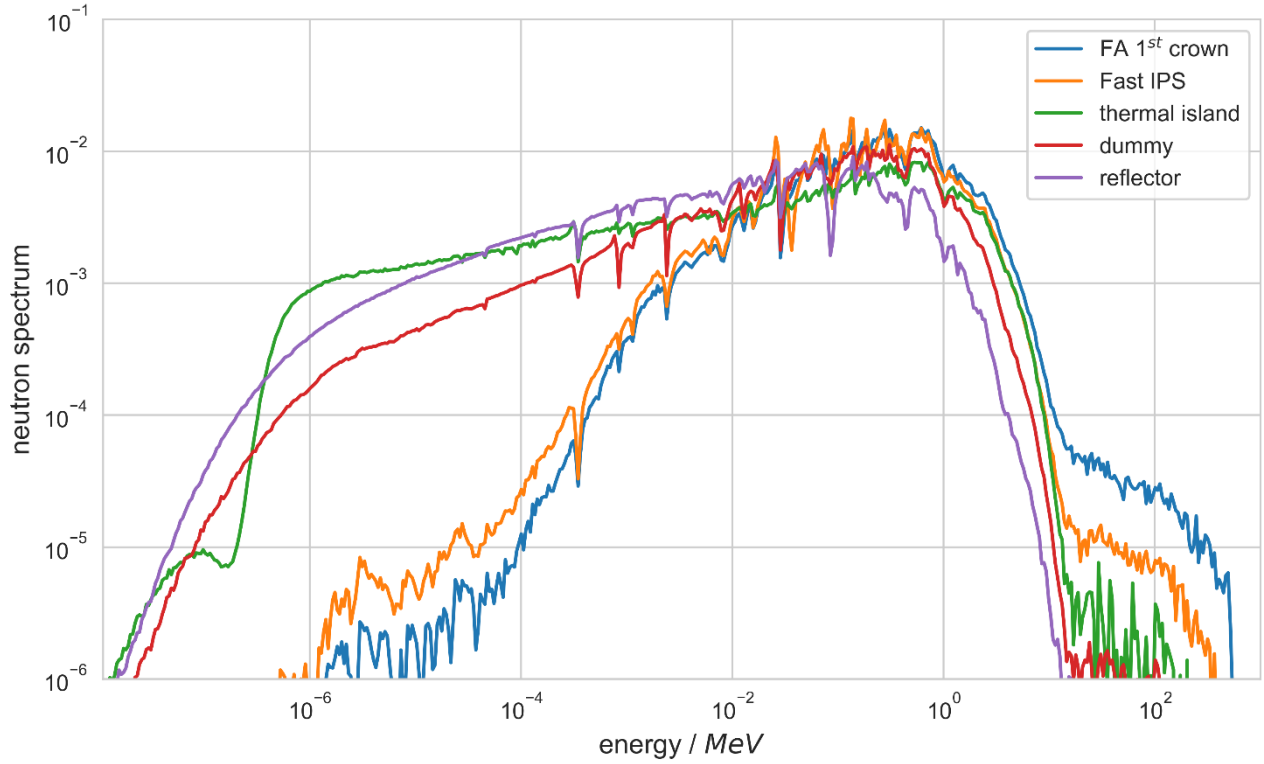

Figure 13: Normalized neutron spectra calculated for the MYRRHA subcritical BoL homogeneous model in several reactor components averaged over the active zone.

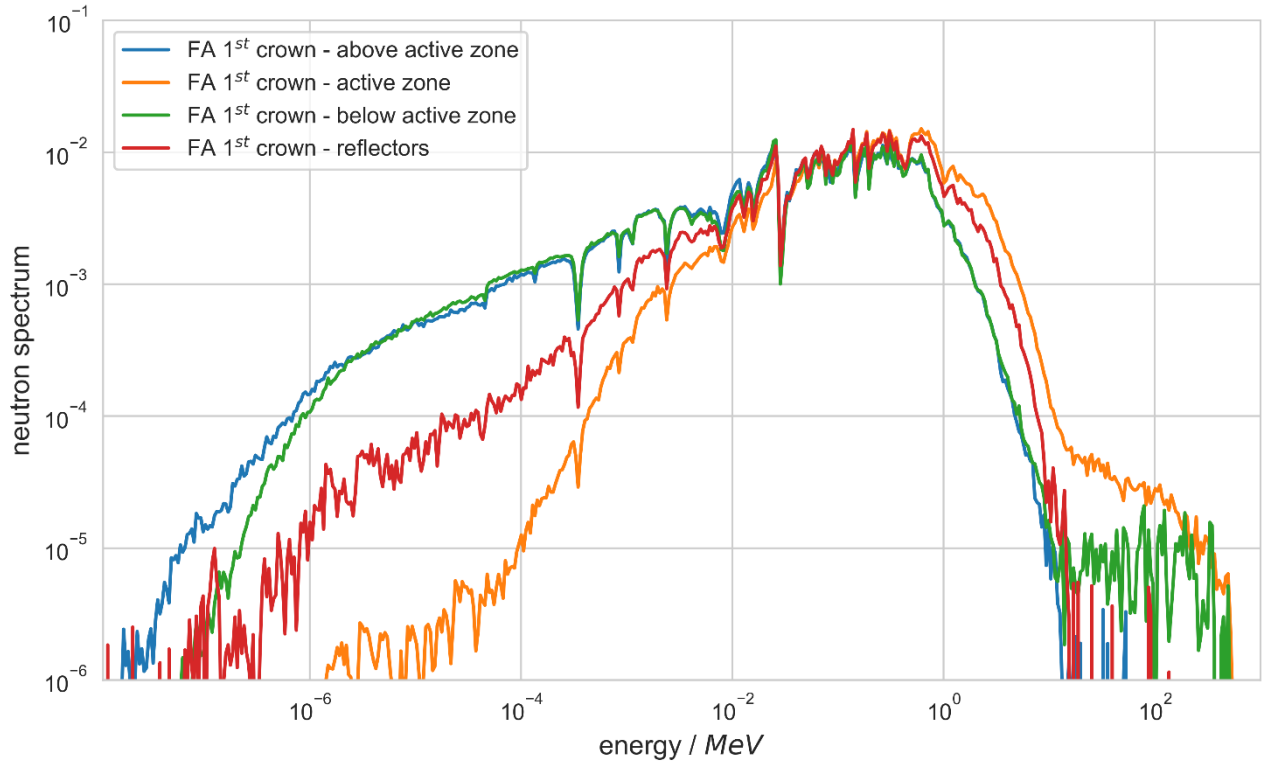

Figure 14: Normalized neutron spectra calculated for the MYRRHA subcritical BoL homogeneous model in a FA in the first crown (batch 101) and averaged over different axial zones.

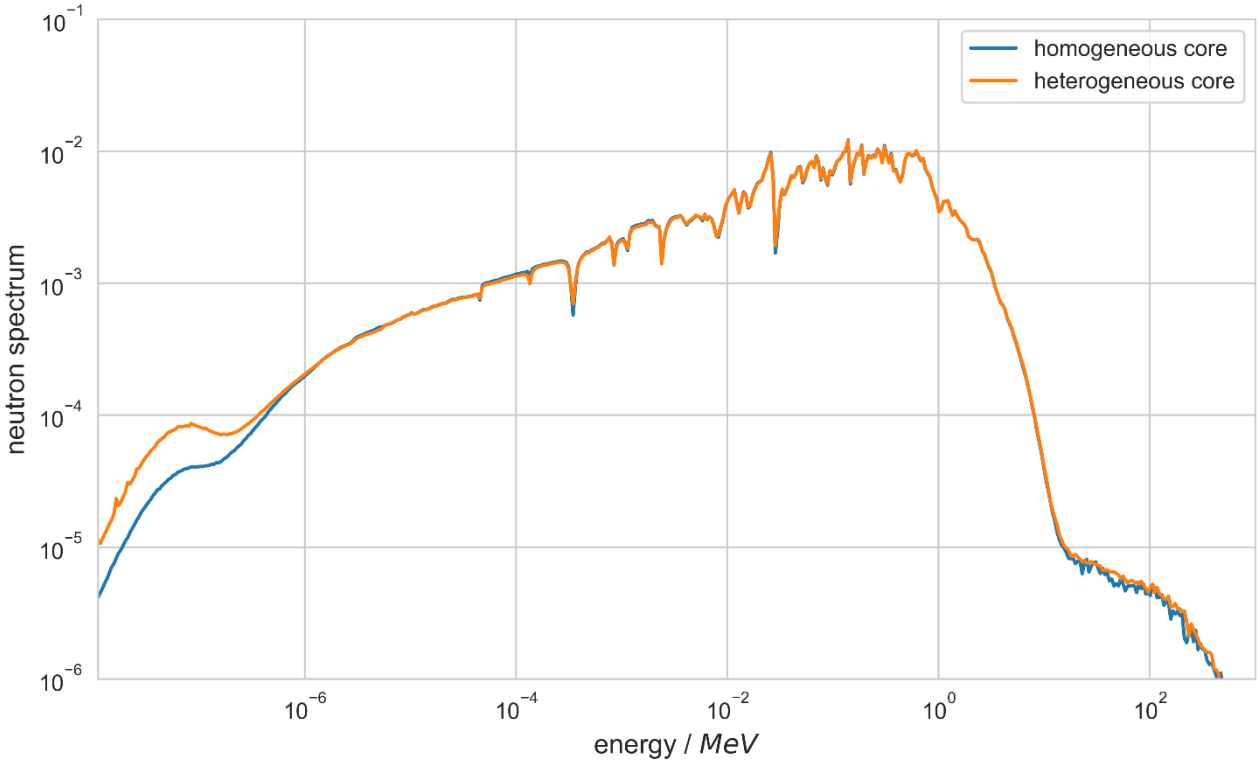

Figure 15: Normalized neutron spectra calculated for the MYRRHA subcritical BoL homogeneous model over the whole core.

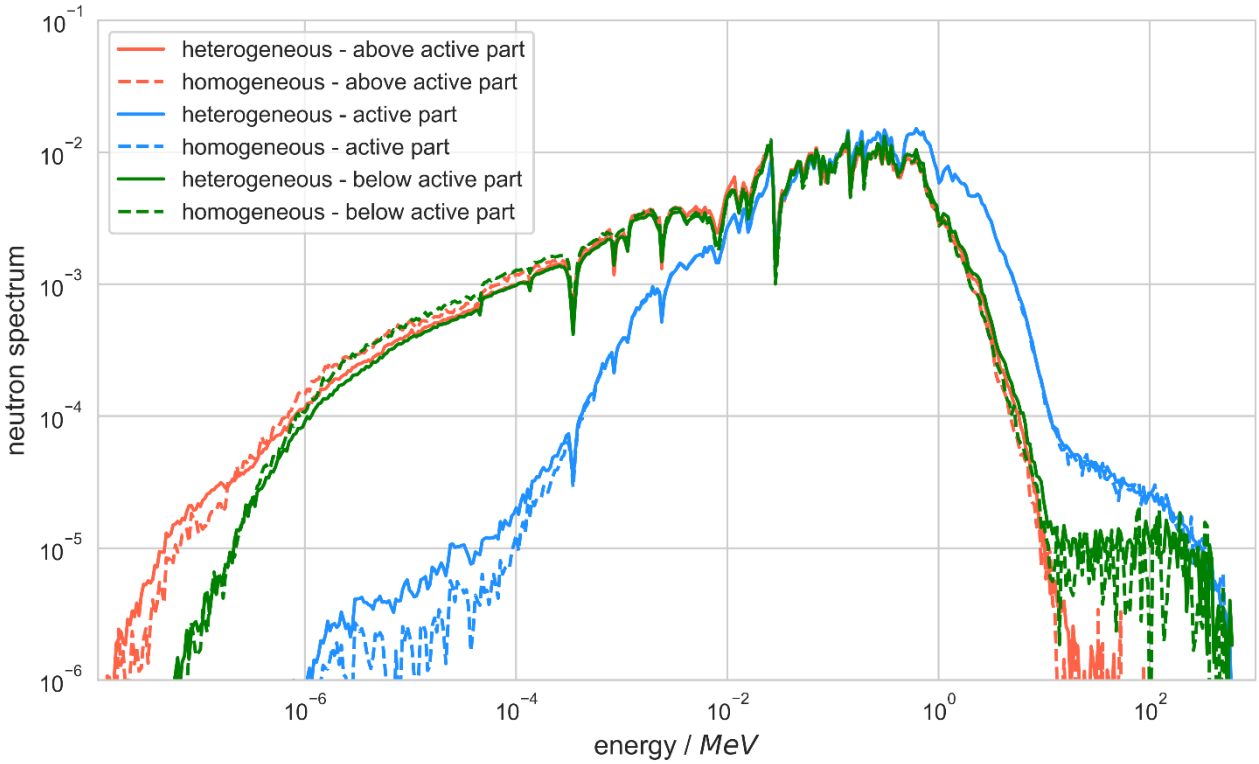

Figure 16: Comparison of the normalized neutron spectra calculated for the MYRRHA subcritical BoL homogenous and heterogeneous models in a FA in the first crown (batch 101) and averaged over different axial zones.

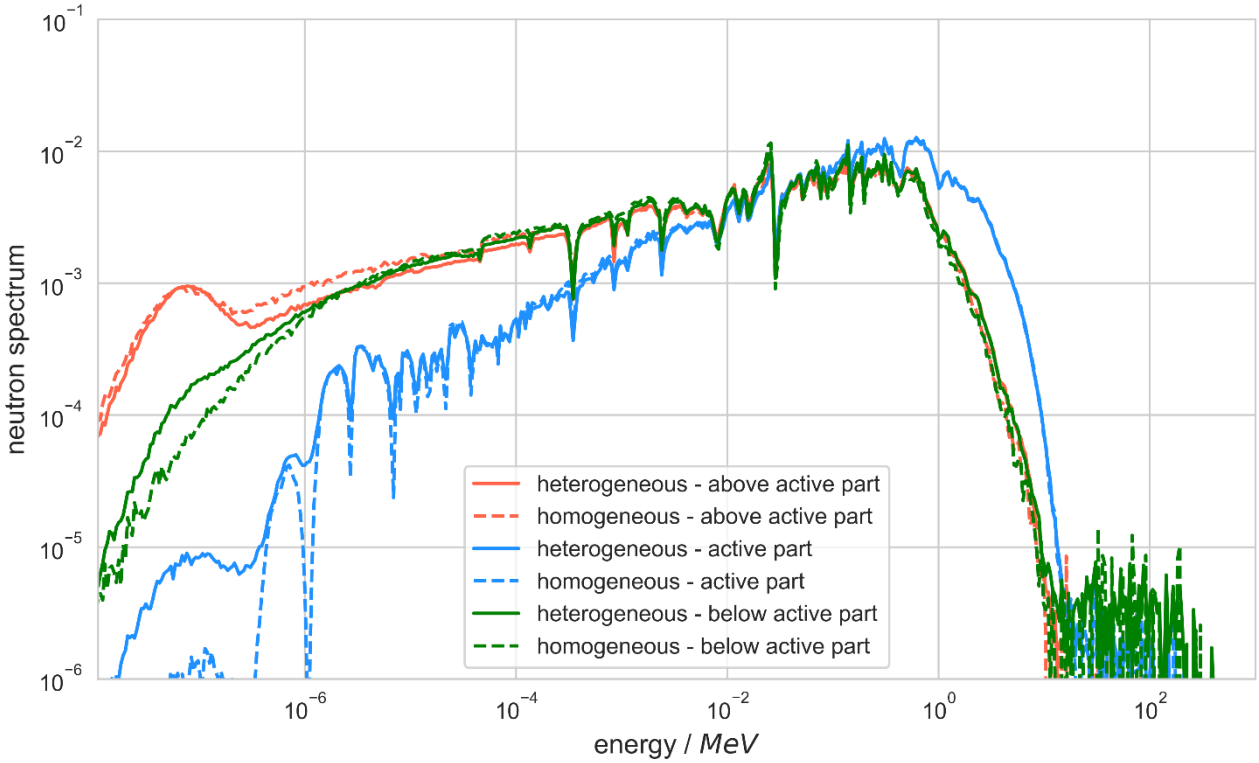

Figure 17: Comparison of the normalized neutron spectra calculated for the MYRRHA subcritical BoL homogenous and heterogeneous models in a FA in the fifth crown (batch 501) and averaged over different axial zones.

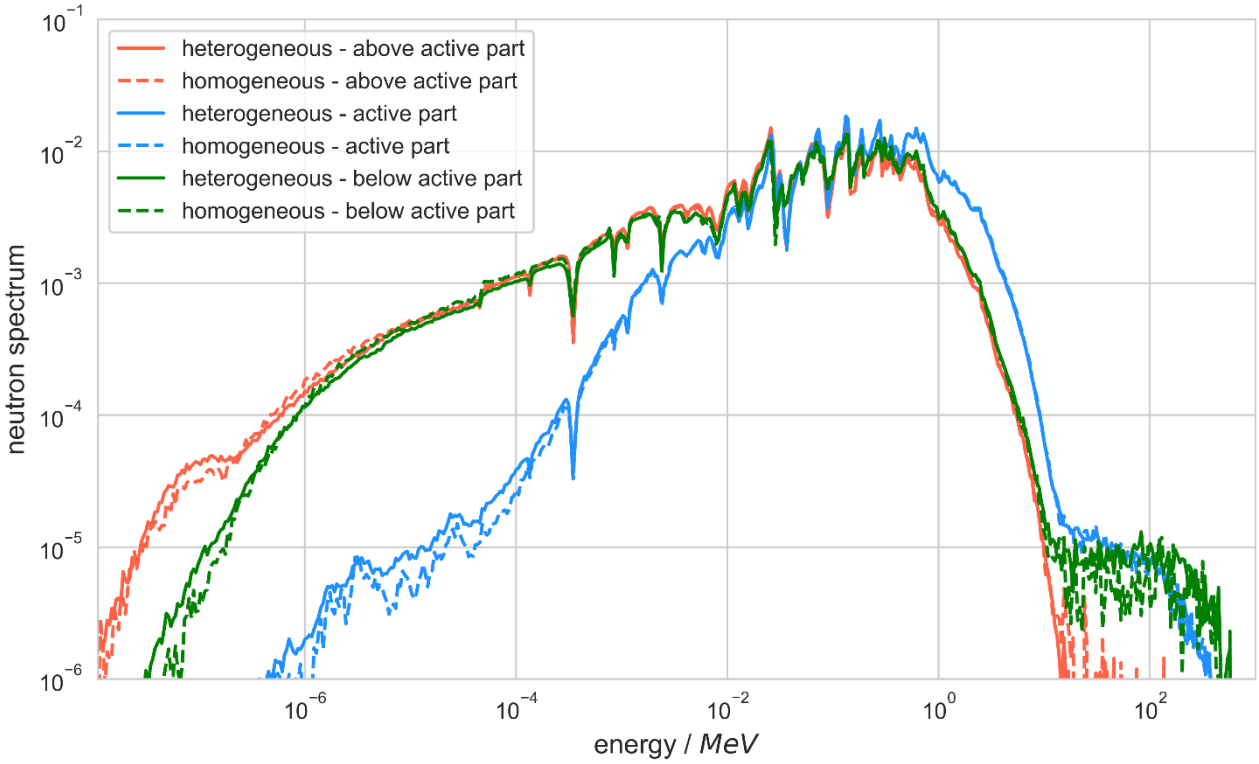

Figure 18: Comparison of the normalized neutron spectra calculated for the MYRRHA subcritical BoL homogenous and heterogeneous models in a fast IPS and averaged over different axial zones.

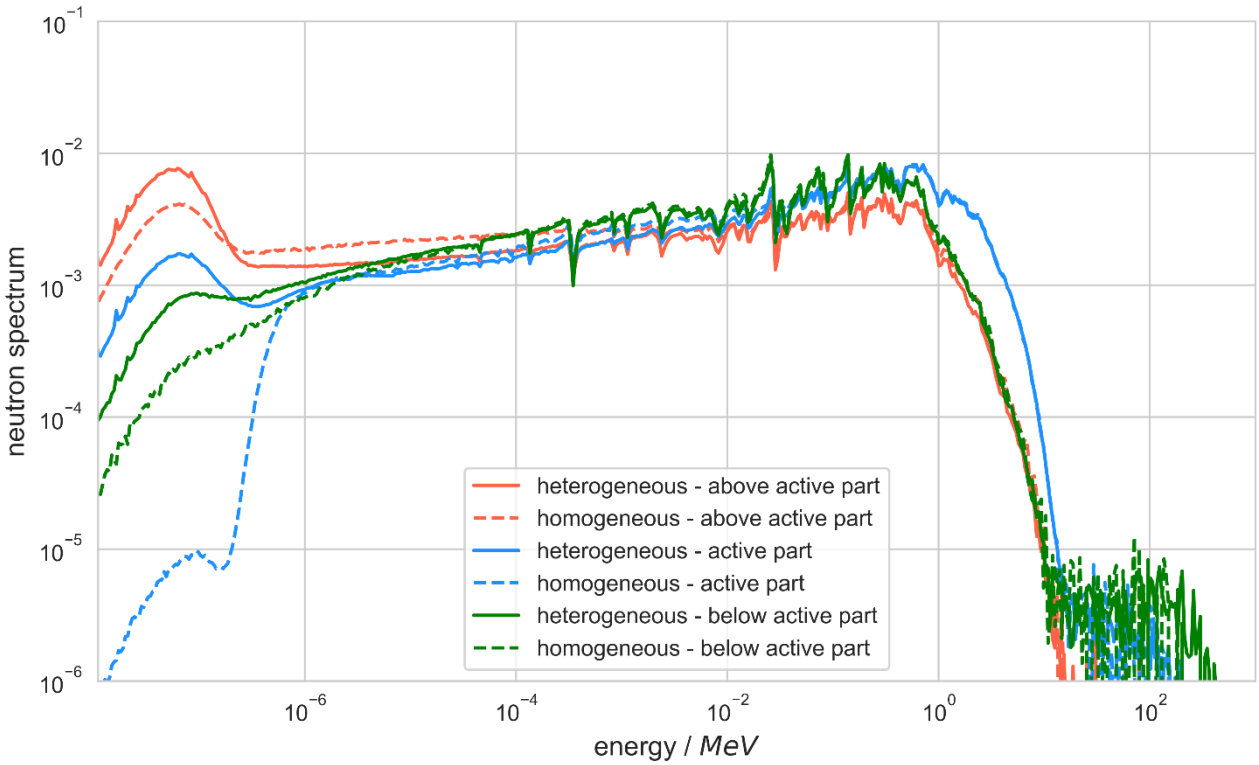

Figure 19: Comparison of the normalized neutron spectra calculated for the MYRRHA subcritical BoL homogenous and heterogeneous models in a thermal island and averaged over different axial zones.

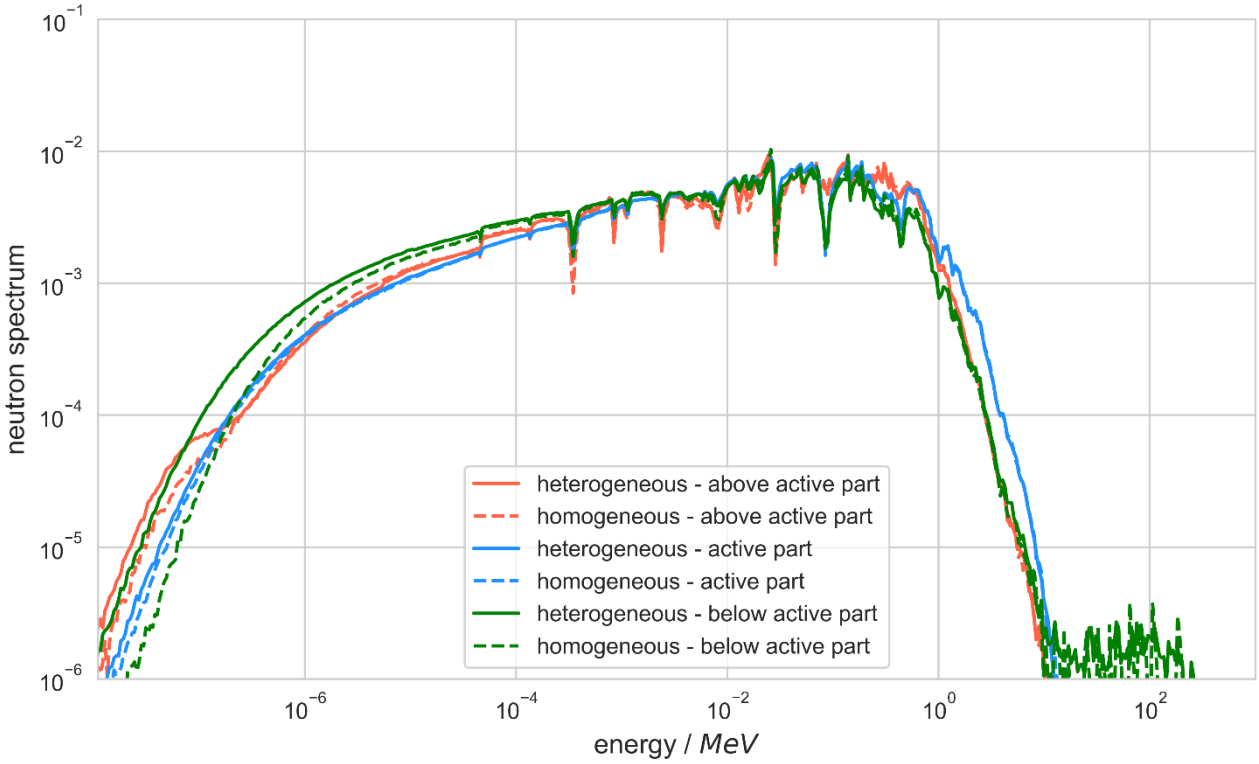

Figure 20: Comparison of the normalized neutron spectra calculated for the MYRRHA subcritical BoL homogenous and heterogeneous models in a reflector assembly and averaged over different axial zones.

References

[1] P. D'Hondt, H. Aït Abderrahim, P. Kupschus, E. Malambu, T. Aoust, P. Benoit, V. Sobolev, K. Van Tichelen, B. Arien, F. Vermeersch, Y. Jongen, S. Ternier, D. Vandeplassche, Pre-design of MYRRHA, A Multipurpose Accelerator Driven System for Research and Development, in: AIP Conf. Proc., American Institute of Physics Inc., 2003: pp. 961–964. https://doi.org/10.1063/1.1619868.

[2] D. De Bruyn, D. Maes, L. Mansani, B. Giraud, From myrrha to XT-ADS: The design evolution of an experimental ADS system, in: AccApp'07, 2007.

[3] D. De Bruyn, P. Baeten, S. Larmignat, A. Woaye Hune, L. Mansani, The FP7 Central Design Team project: Towards a Fast-Spectrum Transmutation Experimental Facility, in: Int. Congr. Adv. Nucl. Power Plants 2010, ICAPP 2010, 2010: pp. 469–475.

[4] H.A. Abderrahim, P. Baeten, B. Neerdael, D. Naidoo, D. De Bruyn, R. Fernandez, G. Van den Eynde, D. Vandeplassche, G. Scheveneels, M. Ottolini, R. Shuff, S. Michiels, MYRRHA Technical Description, 2011.

[5] E. Malambu, G. Van Den Eynde, R. Fernandez, P. Baeten, H. Aït Abderrahim, MA transmutation performance in the optimized MYRRHA, in: Int. Nucl. Fuel Cycle Conf. Glob. 2013 Nucl. Energy a Crossroads, American Nuclear Society, 2013: pp. 775–780.

[6] E. Malambu Mbala, A. Stankovskiy, Revised Core Design for MYRRHA-Rev1 .6, 2014.

[7] A. Stankovskiy, G. Van den Eynde, Neutronic model of MYRRHA design revision 1.6, 2014.

[8] P. Romojaro, F. Álvarez-Velarde, I. Kodeli, A. Stankovskiy, C.J. Díez, O. Cabellos, N. García-Herranz, J. Heyse, P. Schillebeeckx, G. Van den Eynde, G. Žerovnik, Nuclear data sensitivity and uncertainty analysis of effective neutron multiplication factor in various MYRRHA core configurations, Ann. Nucl. Energy. 101 (2017) 330–338. https://doi.org/10.1016/j.anucene.2016.11.027.

[9] I.A. Kodeli, Beta-effective sensitivity and uncertainty analysis of MYRRHA reactor for possible use in nuclear data validation and improvement, Ann. Nucl. Energy. 113 (2018) 425–435. https://doi.org/10.1016/j.anucene.2017.11.039.

[10] G. Zerovnik, F. Alvarez-Velarde, O. Cabellos, L. Fiorito, N. García-Herranz, J. Heyse, I. Kodeli, S. Kopecky, B. Kos, P. Romojaro, P. Schillebeeckx, A. Stankovskiy, G. Van den Eynde, Recommendations for MYRRHA relevant cross section data to the JEFF project, 2017. https://doi.org/10.2760/485552.

[11] A.J.M. Plompen, O. Cabellos, C. De Saint Jean, M. Fleming, A. Algora, M. Angelone, P. Archier, E. Bauge, O. Bersillon, A. Blokhin, F. Cantargi, A. Chebboubi, C. Diez, H. Duarte, E. Dupont, J. Dyrda, B. Erasmus, L. Fiorito, U. Fischer, D. Flammini, D. Foligno, M.R. Gilbert, J.R. Granada, W. Haeck, F.-J. Hambsch, P. Helgesson, S. Hilaire, I. Hill, M. Hursin, R. Ichou, R. Jacqmin, B. Jansky, C. Jouanne, M.A. Kellett, D.H. Kim, H.I. Kim, I. Kodeli, A.J. Koning, A.Y. Konobeyev, S. Kopecky, B. Kos, A. Krása, L.C. Leal, N. Leclaire, P. Leconte, Y.O. Lee, H. Leeb, O. Litaize, M. Majerle, J.I. Márquez Damián, F. Michel-Sendis, R.W. Mills, B. Morillon, G. Noguère, M. Pecchia, S. Pelloni, P. Pereslavtsev, R.J. Perry, D. Rochman, A. Röhrmoser, P. Romain, P. Romojaro, D. Roubtsov, P. Sauvan, P. Schillebeeckx, K.H. Schmidt, O. Serot, S. Simakov, I. Sirakov, H. Sjöstrand, A. Stankovskiy, J.C. Sublet, P. Tamagno, A. Trkov, S. van der Marck, F. Álvarez-Velarde, R. Villari, T.C. Ware, K. Yokoyama, G. Žerovnik, The joint evaluated fission and fusion nuclear data library, JEFF-3.3, Eur. Phys. J. A. 56 (2020) 181. https://doi.org/10.1140/epja/s10050-020-00141-9.

[12] L. Fiorito, Neutronics core design of MYRRHA – version 1.8, 2019.

[13] A.J.M. Plompen, Status of the JEFF-3.3 paper and JEFF-4.0, 2019. https://www.oecd-nea.org/dbdata/nds_jefdoc/jefdoc-1974.pdf.

[14] C.J. Werner, J. Armstrong, F.B. Brown, J.S. Bull, L. Casswell, L.J. Cox, D. Dixon, R.A. Forster, J.T. Goorley, H.G. Hughes, J. Favorite, R. Martz, S.G. Mashnik, M.E. Rising, C. Solomon, A. Sood, J.E. Sweezy, C.J. Werner, A. Zukaitis, C. Anderson, J.S. Elson, J.W. Durkee, R.C. Johns, G.W. McKinney, G.E. McMath, J.S. Hendricks, D.B. Pelowitz, R.E. Prael, T.E. Booth, M.R. James, M.L. Fensin, T.A. Wilcox, B.C. Kiedrowski, MCNP User's Manual Code Version 6.2, 2017.

[15] A. Stankovskiy, G. Van den Eynde, Advanced Method for Calculations of Core Burn-Up, Activation of Structural Materials, and Spallation Products Accumulation in Accelerator-Driven Systems, Sci. Technol. Nucl. Install. 2012 (2012) 1–12. https://doi.org/10.1155/2012/545103.

[16] A.J. Koning, E. Bauge, C.J. Dean, E. Dupont, U. Fischer, R.A. Forrest, R. Jacqmin, H. Leeb, M.A. Kellett, R.W. Mills, C. Nordborg, M. Pescarini, Y. Rugama, P. Rullhusen, Status of the JEFF nuclear data library, J. Korean Phys. Soc. 59 (2011) 1057–1062. https://doi.org/10.3938/jkps.59.1057.

[17] A. Stankovskiy, On the choice of nuclear data library for neutronics design of MYRRHA fast spectrum facility, Mol, 2012.

[18] A. Stankovskiy, Processing of the JEFF-3.1.1, JEFF-3.1.2 and ENDF/B-VII.1 neutron cross section data into multi-temperature continuous energy Monte Carlo radiation transport libraries, Mol, 2012.

[19] S.G. Mashnik, A.J. Sierk, CEM03.03 User Manual, 2012.

[20] A. Stankovskiy, On the choice of intermediate- and high-energy model for MYRRHA sub-critical core neutronics calculations, Mol, 2012.

[21] A. Stankovskiy, Optimization of the beam window position, 2011.

[22] A. Stankovskiy, G. Van Den Eynde, L. Fiorito, ALEPH A Monte Carlo Depletion Code – Version 2.8 User's Manual, 2021.

[23] P.K. Romano, B. Forget, The OpenMC Monte Carlo particle transport code, Ann. Nucl. Energy. 51 (2013) 274–281. https://doi.org/10.1016/j.anucene.2012.06.040.

[24] P.K. Romano, N.E. Horelik, B.R. Herman, A.G. Nelson, B. Forget, K. Smith, OpenMC: A state-of-the-art Monte Carlo code for research and development, Ann. Nucl. Energy. 82 (2015) 90–97. https://doi.org/10.1016/j.anucene.2014.07.048.

[25] Y. Molla, OPENMC MODELING OF THE CRITICAL MYRRHA CONFIGURATION: AN EMPHASIS IN CROSS SECTION HOMOGENIZATION, LAPPEENRANTA-LAHTI UNIVERSITY OF TECHNOLOGY LUT, 2020.